Growth variation effects in SiGe-based quantum cascade lasers

A. Valavanis, Z. Ikonić and R. W. Kelsall

Institute of Microwaves and Photonics, School of Electronic and Electrical Engineering, University of Leeds, Woodhouse Lane, Leeds LS2 9JT, UK

E-mail: `a.valavanis05@leeds.ac.uk`

Abstract. Epitaxial growth of SiGe quantum cascade (QC) lasers has thus far proved difficult, and nonabrupt Ge profiles are known to exist. We model the resulting barrier degradation by simulating annealing in pairs of quantum wells (QWs). Using a semi-classical charge transport model, we calculate the changes in scattering rates and transition energy between the lowest pair of subbands.

We compare results for each of the possible material configurations for SiGe QC lasers. The effects are most severe in n- type (001) Si-rich systems due to the large effective electron mass, and in p-type systems due to the coexistence of light- and heavy-holes.

The lower effective mass and conduction band offset of (111) oriented systems minimises transition energy variation, and a large interdiffusion length ($L_d = 1.49\,\text{nm}$) is tolerated with respect to scattering rate. Ge-rich systems are shown to give the best tolerance with respect to subband separation ($L_d = 3.31\,\text{nm}$), due also to their low effective mass.

1. Introduction

SiGe-based QC lasers present several possible advantages over III-V materials. These include a possible route toward CMOS/photonic integrated circuits and high temperature operation due to the greater thermal conductivity and the absence of polar LO-phonon interactions.[1]

The electronic behaviour of such devices varies significantly depending on alloy composition, the doping (n- or p-type) and crystal orientation. Electroluminescence has been observed in p-type Si-rich (001) oriented QC structures,[2, 3] but lasing remains an elusive goal. Improving the design of p-type QC lasers is difficult due to the coexistence

of light-hole (LH) and heavy-hole (HH) states. This causes fast nonradiative scattering and large variations in transition energies and matrix elements with in-plane wave vector.[4]

n-type Si-rich (001) oriented structures are adversely affected by the large longitudinal effective mass of the SiGe Δ-valleys.[5] This gives a low gain coefficient and requires very thin layers to achieve quantum confinement. Alternative approaches, which avoid this problem include either moving to the (111) crystal orientation[6] or using the *L*-valleys in Ge-rich systems.[7]

Charge transport simulations typically assume that abrupt changes in alloy composition are possible.[8] In reality however, diffuse Ge profiles may result from processes such as surface segregation during growth,[9] or by annealing.[10] Having established that this leads to significant changes in the subband spacing and scattering rates in QWs,[11] we now turn to the specific issue of barrier degradation in QC lasers.

In this paper, we consider a single barrier separating a pair of QWs. We compare its degradation in each material configuration in order to estimate the effect on QC laser performance. In the following sections, we briefly summarise our semiclassical transport model and the general effect of interdiffusion upon semiconductor bandstructure. We then define figures of merit for tolerance to Ge interdiffusion and use the method proposed in our previous work[11] to investigate the degradation in barrier potential for coupled QWs in each of the material configurations discussed above.

2. Theoretical method

2.1. Diffuse bandstructure

We calculated the conduction band potential for SiGe heterostructures using a model solid approximation,[12] accounting for strain effects and crystal orientation.[13, 14] A one-band effective mass approximation was used to calculate the band structure for *n*-type heterostructures, whereas a 6×6 $\mathbf{k} \cdot \mathbf{p}$ calculation[8] was used to account for the coexistence of LH and HH states in *p*-type systems.

Surface segregation yields asymmetric Ge interdiffusion profiles, as Ge preferentially rises to the surface during epitaxial growth.[9] In contrast, annealing leads to symmetric interdiffusion, as it depends only upon the concentration difference at interfaces.[10] Both processes change the electronic behaviour of a system by narrowing the QWs, degrading the barriers and reducing the purity of material within the QWs. Due to this intrinsic similarity between the processes, we approximate their combined effect as resulting from a single annealing-like process characterised by an effective diffusion length L_d.[10] Diffusion lengths around $L_d \approx$ 1–2 nm have been observed experimentally.[15]

In this work, we consider pairs of coupled QWs with 22% variation in the Ge fraction at interfaces. For the *n*-type Si-rich systems, we simulated pure Si wells with 22% Ge barriers. As SiGe alloys are type-II semiconductors,[16] the well and barrier
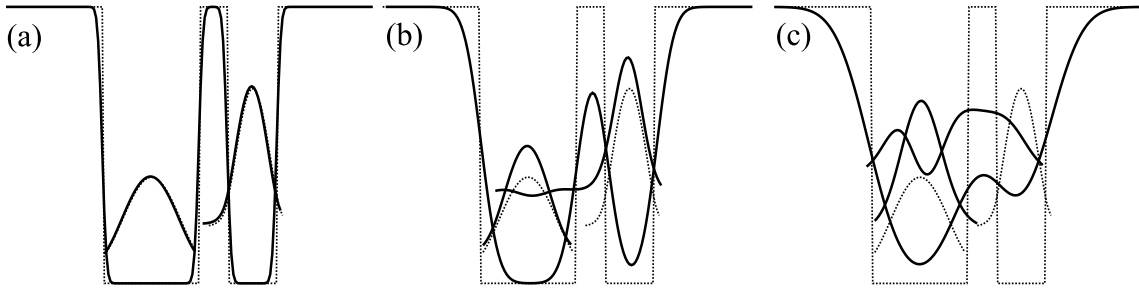
Figure 1. Conduction band potential and lowest two subband minima shown schematically (solid lines) for varying degrees of interdiffusion. The nominal values are shown as dotted lines in each plot. (a) shows the "uncoupled" regime, corresponding to low interdiffusion. (b) shows the weak coupling regime, in which interdiffusion degrades the barrier between wells. (c) shows the "single well" regime, in which large interdiffusion merges the wells.

materials were swapped over for the *p*-type structure. For the Ge-rich system, pure Ge wells with 22% Si barriers were used.

We initially considered an *n*-type (001) oriented Si-rich structure with well widths of 5 and 2.5 nm separated by a 1.5 nm barrier. The resulting energy separation between the lowest pair of subbands is 20 meV. The lower energy electrons are strongly confined in the wider well, and the higher energy electrons in the narrower well as shown in figure 1(a). Subsequent structures were obtained by scaling layer widths l by the factor

$$l' = l\sqrt{\frac{m_q}{m_q'}}, \tag{1}$$

where m_q is the quantisation effective mass, and the prime symbol denotes parameters for the new system. This scaling factor provides an exact match of subband spacing for infinitely deep quantum wells. However, as finite quantum wells are considered in this work, the energy of the upper subband is reduced slightly. To compensate, the width of the smaller well was "tuned" to increase the subband spacing to 20 meV as required.

Specific results for each material configuration are discussed in the following sections, but some general characteristics of diffuse double quantum well systems may be identified. Figure 1 shows the results for the (001) oriented *n*-type Si rich system described above. Three distinct regimes can be identified, as interdiffusion increases. For low interdiffusion [figure 1(a)] the interfaces are almost abrupt, and the barrier is well defined. This effectively uncouples the wells, resulting in very small overlap between the lowest pair of subbands.

As interdiffusion increases, the barrier degrades [figure 1(b)] and the wells become weakly coupled, leading to an increased overlap between subbands. The bottoms of the wells narrow, leading to a an increased subband spacing. At very large interdiffusion lengths,[figure 1(c)] the barrier potential is substantially reduced, and the system resembles a single quantum well with the nominal "barrier" region acting as a perturbation. The region of overlap between subbands now extends across the entire
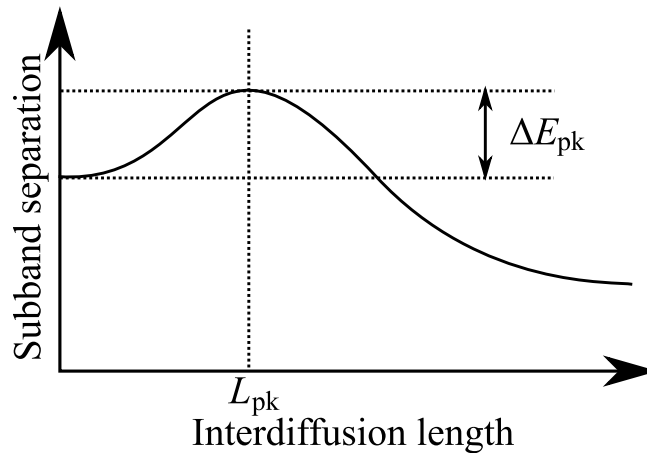
Figure 2. Schematic representation of subband spacing as a function of interdiffusion length. In the "weak coupling" regime ($L_d < L_{pk}$), the subband spacing increases to a peak shift of ΔE_{pk}. At greater interdiffusion lengths, the subband spacing decreases.

system, and the energy spacing between subbands is determined approximately by the width of the wide, single well and is hence lower than the nominal value.

2.2. Transport model

Having calculated the bandstructure, we determined the average scattering rate from upper to lower subband. We used a semiclassical time-independent perturbation theoretical approach, including interface roughness (IR), alloy disorder (AD), deformation potential electron–phonon interactions (EP), acoustic phonon (AC) and ionised impurity (II) interactions.[11]

For all our calculations, we set the lattice temperature to $4\,\mathrm{K}$. The carrier temperature was set to $24\,\mathrm{K}$ which yields scattering rates in good agreement with pump-probe spectroscopy measurements on double well systems.[17] As modulation doping of SiGe-based heterostructures may be poor,[9] doping was spread evenly throughout each system at a concentration of $10^{16}\,\mathrm{cm^{-3}}$. The resulting space charge distribution was found (using a self-consistent Poisson-Schrödinger calculation) to cause negligible band bending effects.

2.3. Figures of merit

To provide a useful comparison between the material configurations, we define three figures of merit for the tolerance to interdiffusion.

Figure 2 gives a schematic representation of the effect on subband spacing described in section 2.1. A pair of figures of merit characterise such an effect. L_{pk} is the interdiffusion length which results in a peak shift in subband separation ΔE_{pk}. L_{pk} is therefore an indicator of the point at which the system moves into the "single well" regime. As this represents a large change in electronic behaviour, it is desirable to
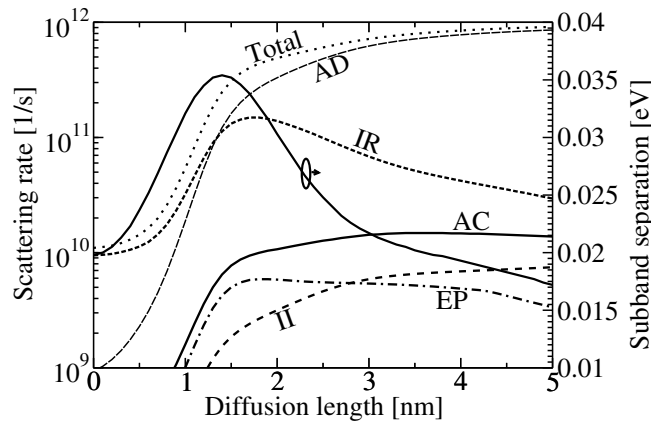
Figure 3. Average scattering rates from second to first subband in an n-type Si-rich (001) oriented double QW system

maximise the value of L_{pk}. Shifts in subband spacing are undesirable in a practical device, and a low value of ΔE_{pk} is preferable. A normalised value $\varepsilon = \frac{\Delta E_{pk}}{E_0}$ gives the peak subband spacing relative to the nominal value.

As stated previously, the overlap between subband states increases as the barrier degrades and this causes an increase in scattering rates. We therefore define a final figure of merit L_w, which is the interdiffusion length which yields a "catastrophic" 50% increase in intersubband scattering rate. An ideal system would maximise this value.

3. Simulation results

3.1. n-type (001) oriented Si-rich structures

In bulk $Si_{1-x}Ge_x$ with $x < 85\%$, the edge of the conduction band is located in the six Δ valleys in reciprocal space.[16] In (001) oriented heterostructures, strain breaks the valley degeneracy and the conduction band edge lies in the two Δ_z valleys (with their major axes in reciprocal space aligned with the growth direction).[13]

The quantisation effective mass of these valleys is $m_q = 0.916$. This is considerably higher than the values for the other material configurations we consider, and hence the layer thicknesses are minimised. The effect of interdiffusion on the geometry of the system is therefore maximised.

Figure 3 shows the calculated intersubband scattering rates and energy separation for an n-type (001) oriented Si-rich structure. A large increase in subband spacing is visible even at small diffusion lengths, leading to a peak shift of $\varepsilon = 1.75$ at $L_{pk} = 1.41$ nm.

At low interdiffusion lengths, IR scattering dominates strongly as all other rates are minimised. II interactions are negligible due to the very small overlap between states and the large energy spacing. AD scattering is minimised as the wells contain pure Si. We make the assumption that the Δ_z valleys are sufficiently low in energy that they
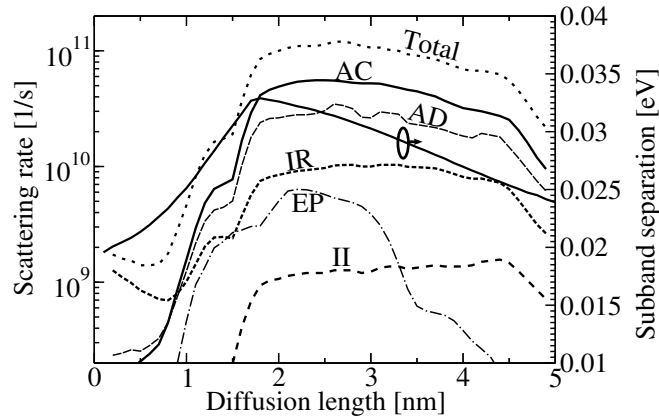
Figure 4. Average scattering rates from second to first subband in a *p*-type Si-rich (001) oriented double QW system

contain the entire carrier population. EP scattering is therefore restricted to *g*-type processes transferring electrons between the two Δ_z valleys. At small interdiffusion lengths, these are limited by the low overlap between states.

Increases in interdiffusion in the weak coupling regime result in a greater overlap between wavefunctions, which causes all scattering rates to rise sharply. A 50% increase in total scattering rate is seen at $L_w = 1.27\,\text{nm}$.

In the "single well" regime, the large Ge fraction in the wells leads to the AD scattering becoming dominant. Simultaneously, the IR scattering decreases as the central barrier decays and the total scattering rate becomes approximately constant. The electronic behaviour of the device therefore shifts from being dominated by IR in the "weak coupling" regime to AD in the "single well" regime.

3.2. *p-type (001) oriented Si-rich structures*

Figure 4 shows the effect of interdiffusion on average scattering rates and subband separation in a *p*-type structure. The difference in effective mass between LH and HH states leads to a pair of overlapping dispersion relations, which causes anticrossing effects between subbands.

For the nominal structure, the first and second subbands both have HH character at $k_{\parallel} = 0$. However, as interdiffusion increases in the weak coupling regime, the second subband (localised in the narrower well) increases in energy. At $L_d = 1.79\,\text{nm}$ an anticrossing occurs and the second subband abruptly switches to LH character and becomes localised in the wider well. Further interdiffusion decreases the Ge fraction in the wider well and hence the strain. The splitting between LH and HH states is consequently reduced. The anticrossing therefore represents the peak subband spacing of $\varepsilon = 1.65$ at $L_{\text{pk}} = 1.79\,\text{nm}$.

The scattering rates also vary in a complex manner. As with the *n*-type system in the previous section, the IR scattering dominates in the absence of interdiffusion. Slight
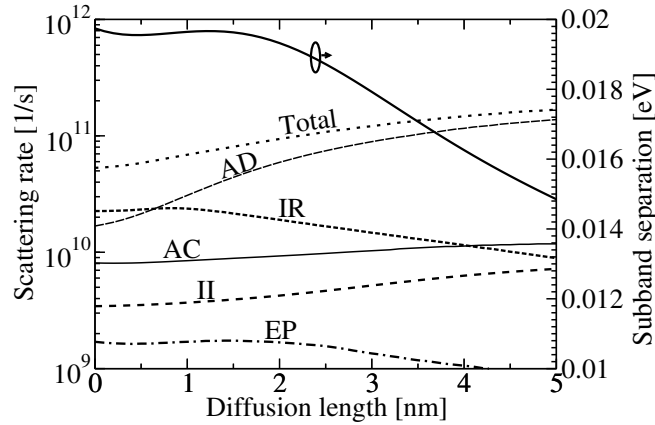
Figure 5. Average scattering rates from second to first subband in a n-type Si-rich (111) oriented double QW system

increases in interdiffusion lead to a reduction in the barrier potential and consequently a reduction in the scattering rate.

As the confining potential is considerably lower in the valence band (150 meV vs. 375 meV), the coupling between the wells increases rapidly with interdiffusion. In the weak coupling regime, the matrix elements for all scattering interactions increase dramatically, giving $L_w = 0.94$ nm. An additional jump in scattering rates occurs at $L_d = L_{pk}$, as the upper subband shifts to LH character.

3.3. n-type (111) oriented Si-rich structures

By moving to the (111) crystal orientation, the quantisation effective mass in a two-dimensional heterostructure is reduced to $0.26\,m_e$,[18] and the required layer thickness is greater than that in (001) structures. The effect of interdiffusion on the geometry of the wider well is therefore relatively small and the lower subband energy is only shifted slightly upward. Additionally, the upper subband lies midway between the well and barrier potentials, where the effect of interdiffusion is minimised. Figure 5 shows that there is very little variation in subband spacing until the single well regime is reached, giving $\varepsilon = 0.99$ at $L_{pk} = 1.37$ nm.

As usual, interdiffusion leads to a switch in dominance between IR and AD scattering, although the large layer widths reduce the effect of interdiffusion upon the geometry and hence slow the switch between mechanisms. The low conduction band offset of 55 meV allows some coupling between the wells, even in the absence of interdiffusion. The sudden appearance of EP and II interactions seen in the (001) oriented system is therefore avoided. This fairly constant background level of scattering interactions, combined with the smooth transition between IR and AD scattering gives a stable total scattering rate with respect to interdiffusion. The corresponding figure of merit $L_w = 1.49$ nm is superior to that of $n-$ and $p-$type Si rich systems in the (001) orientation.
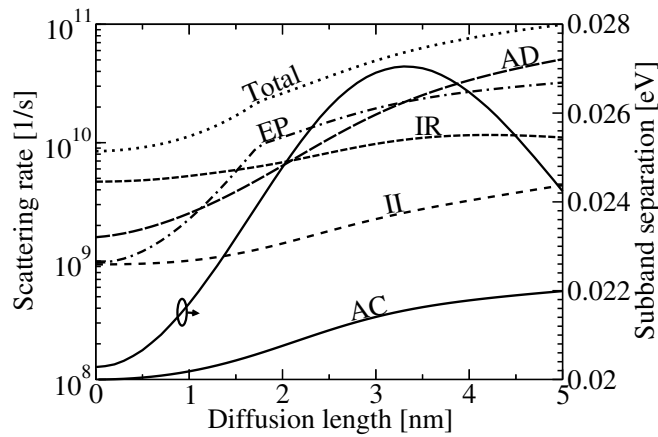
Figure 6. Average scattering rates from second to first subband in a n-type Ge-rich (001) oriented double QW system

3.4. n-type (001) oriented Ge-rich structures

The final set of results is shown in figure 6, for a (001) oriented n-type Ge rich system. Due to the large Ge fraction, the conduction band edge is located in the L-valleys in reciprocal space, which results in an effective mass of $m_q = 0.12\,m_e$,[13] which is the lowest of the systems considered in this work. The layer widths are therefore large, and the amount of interdiffusion required for single well behaviour is large, giving $L_{pk} = 3.31\,\text{nm}$. Although the weak coupling regime persists over a large range of interdiffusion lengths, the subband separation is shown to rise more than in (111) oriented Si-rich systems, giving $\varepsilon = 1.35$. This occurs because the conduction band offset of 95 meV is larger than that of (111) oriented Si and the upper subband lies below the midpoint of the well and barrier potentials. The upper subband is therefore affected more strongly by the narrowing of the bottom of the well than in (111) oriented Si.

As usual, a transition between IR and AD scattering dominance is seen, although the rate of change of scattering rates is reduced due to the large layer widths. The effect of the gradual reduction in interface potential is exceeded by the increase in overlap between the subbands. This results in a slight increase in IR scattering and the "balancing" of the IR and AD scattering rates is not achieved.

Additionally, intervalley electron–phonon interactions are significant due to the large deformation potential ($D_0 = 5.26 \times 10^8\,\text{eV/cm}$ in Ge[19] c.f. $3.4 \times 10^8\,\text{eV/cm}$ in Si[20]). The scattering rate increases for small amounts of interdiffusion, as the subband spacing approaches the phonon energy of 23.95 meV.[19] For subband separation around this value, the EP interactions become the dominant scattering process. As subband spacing increases above the phonon energy, the overlap between subbands leads to a further, gradual increase in EP scattering, although AD scattering regains dominance in the single well regime.

The combination of these effects leads to a faster increase in the total scattering than

Table 1. Comparison between figures of merit for each material configuration.

System	L_{pk} [nm]	ε	L_{w} [nm]
n-type (001) Si	1.41	1.75	1.27
p-type (001) Si	1.79	1.65	0.91
n-type (111) Si	1.37	0.99	1.49
n-type (001) Ge	3.31	1.35	1.21

that seen in the (111) oriented Si-rich system. Consequently, the level of interdiffusion required for a 50% increase in scattering $L_{\mathrm{w}} = 1.21\,\mathrm{nm}$, is slightly lower.

4. Conclusion

We have compared barrier degradation due to Ge interdiffusion in each of the possible material configurations for QC lasers. We defined a set of figures of merit to describe the tolerance of each configuration to interdiffusion, with respect to subband separation and total scattering rate. The calculated values for these figures of merit are compared in table 1.

In general, we have shown for all material configurations, that interface roughness makes a greater contribution than alloy disorder to the total scattering rate in systems with abrupt interfaces. The converse is true for diffuse systems. As interdiffusion increases, the total scattering rate becomes larger due to increased overlap between subbands.

The subband spacing varies in a more complicated manner. Small levels of interdiffusion lead to a "weak coupling" regime, in which the bottoms of the wells become narrower and subband separation increases. Larger levels of interdiffusion cause the system to behave more like a single QW, and the subband separation decreases.

Our results support earlier conclusions[5] that n-type (001) oriented Si-rich systems are poorly suited to QC laser design. However, we have also shown that p-type systems may also be intolerant to interdiffusion. Scattering in p-type systems is badly affected by interdiffusion, due to anticrossings between light- and heavy-hole states. In a QC laser, this could lead to the creation of scattering pathways which deviate significantly from the design. We therefore expect population inversion (and hence lasing) to require almost perfectly abrupt interfaces ($L_d < 0.91\,\mathrm{nm}$) in p-type systems.

We have shown that the tolerance of n-type QC lasers to interdiffusion may be improved by moving to the (111) orientation or by using Ge quantum wells. The low effective mass of these systems allows thicker layers to be used and the effect of interdiffusion on their geometry is less severe. The conduction band offset in (111) oriented systems is lower than that in Ge-rich systems and we have shown that this leads to (111) oriented systems showing almost no variation in their subband spacing for small amounts of interdiffusion. An improvement in the stability of scattering processes is also achievable, giving $L_w < 1.49\,\mathrm{nm}$.

Ge-rich systems show a moderate improvement in the stability of subband spacing at low interdiffusion lengths. However, we have shown that a significant barrier potential exists up to very large interdiffusion lengths ($L_d < 3.31\,\text{nm}$). Finally, our results show that care must be taken in Ge-rich systems due to the rapid electron–phonon interactions for subbands separated by more than 24 meV. By avoiding transitions just below the phonon energy in QC laser designs, we expect that much better stability of scattering rates may be achieved.

Acknowledgments

References

[1] Kelsall R W, Ikonić Z, Harrison P, Lynch S A, Bates R, Paul D J, Norris D J, Liew S L, Cullis A G, Robbins D J, Murzyn P, Pidgeon C R, Arnone D D and Soref R A 2003 *Towards the First Silicon Laser* (*NATO Science Series II: Mathematics, Physics and Chemistry* vol 93) ed Pavesi L, Gaponenko S and Negro L D (Kluwer Academic Publishers, Dordrecht) pp 367–382

[2] Dehlinger G, Diehl L, Gennser U, Sigg H, Faist J, Ensslin K, Grutzmacher D and Muller E 2000 *Science* **290** 2277–2280

[3] Bates R, Lynch S, Paul D, Ikonić Z, Kelsall R, Harrison P, Liew S, Norris D, Cullis A, Tribe W and Arnone D 2003 *Appl. Phys. Lett.* **83** 4092–4094

[4] Ikonić Z, Harrison P and Kelsall R W 2001 *Phys. Rev. B* **64** 245311

[5] Paul D J 2004 *Semicond. Sci. Tech.* **19** R75–R108

[6] Lever L, Valavanis A, Ikonić Z and Kelsall R W 2008 *Appl. Phys. Lett.* **92** 021124

[7] Driscoll K and Paiella R 2006 *Appl. Phys. Lett.* **89** 191110

[8] Ikonic Z, Harrison P and Kelsall R W 2004 *J. Appl. Phys.* **96** 6803–6811

[9] Zhang J, Turner S, Chiam S, Liu R, Tok E, Wee A, Huan A, Kelly I and Mulcahy C 2006 *Surf. Sci.* **600** 2288

[10] Li E H, Weiss B L and Chan K S 1996 *IEEE J. Quantum. Electron.* **32** 1399–1416

[11] Valavanis A, Ikonić Z and Kelsall R W 2008 *Phys. Rev. B* **77**(7) 075312

[12] Van de Walle C G 1989 *Phys. Rev. B* **39** 1871–1883

[13] Smirnov S and Kosina H 2004 *Solid State Electron.* **48** 1325–1335

[14] Valavanis A, Lever L, Evans C A, Ikonić Z and Kelsall R W 2008 *Phys. Rev. B* **78** 035420 (pages 7)

[15] Ozguven N and McIntyre P C 2008 *Appl. Phys. Lett.* **92** 181907 (pages 3)

[16] Rieger M M and Vogl P 1993 *Phys. Rev. B* **48** 14276–14287

[17] Califano M, Vinh N Q, Phillips P J, Ikonic Z, Kelsall R W, Harrison P, Pidgeon C R, Murdin B N, Paul D J, Townsend P, Zhang J, Ross I M and Cullis A G 2007 *Phys. Rev. B* **75** 045338

[18] Rahman A, Lundstrom M S and Ghosh A W 2005 *J. Appl. Phys.* **97** 053702–1–11

[19] Fischetti M 1991 *IEEE Transactions on Electron Devices* **38** 634–649 ISSN 0018-9383

[20] Dollfus P 1997 *J. Appl. Phys.* **82** 3911–3916